International Journal of Automotive Technology, Vol. 8, No. 4, pp. 467–476 (2007)

1229–9138/2007/035–09

ON CONTROLLING A CHAOTIC VEHICLE DYNAMIC SYSTEM BY USING DITHER

S.-C. CHANG*

Department of Mechanical and Automation Engineering, Dayeh University, Taiwan 51591, Republic Of China

(Received 6 November 2006: Revised 30 June 2007)

ABSTRACT–This work verifies the chaotic motion of a steer-by-wire vehicle dynamic system, and then elucidates an application of dither smoothing to control the chaos of a vehicle model. The largest Lyapunov exponent is estimated from the synchronization to identify periodic and chaotic motions. Then, a bifurcation diagram reveals complex nonlinear behaviors over a range of parameter values. Finally, a method for controlling a chaotic vehicle dynamic system is proposed. This method involves applying another external input, called a dither signal, to the system. The designed controller is demonstrated to work quite well for nonlinear systems in achieving robust stability and protecting the vehicle from slip or spin. Some simulation results are presented to establish the feasibility of the proposed method.

KEY WORDS : Chaos, Steer-by-wire, Synchronization, Lyapunov exponent, Dither

1. INTRODUCTION

The steering control of vehicles has attracted much attention in recent years (Shibahata *et al.*, 1986; Takiguchi *et al.*, 1986; Sano *et al.*, 1986; Ackermann and Sienel, 1993). This control is introduced to improve the stability and maneuverability of a vehicle under all driving conditions. In particular vehicle steering control should improve the safety of critical cornering behaviors in an emergency. As the driving conditions change from moderate cornering on a dry road to hard cornering on a low-friction road, the dynamics may display unstable characteristics. In the worst case, the vehicle will fall into a spin. To control vehicle handling dynamics, numerous approaches have recently been proposed, including those by Harada and Harada (1999), Catino *et al.* (2003), and You and Jeong (2002). However, the stability analysis of the system presented in their studies was based on an assumption of linear tire-side force characteristics even though that linear relationship applies only locally.

When the steering system moves the front wheels in response to driver command inputs in order to provide overall directional control of the vehicle, that system consists of a handling mechanism, steering gear and steering linkage. It has a mechanical connection between the driver and the front wheels. However, a steer-by-wire system has no mechanical steering column. In this way, many traditional constraints are eliminated. Several projects have been undertaken to study the control of vehicle handling using a steer-by-wire system (Yih and Gerdes, 2005; Hayama and Nishizaki, 2000; Segawa *et al.*, 2001; Setlur *et al.*, 2002; Hosaka and Murakami, 2004). Only Yih and Gerdes (2005) have discussed the handling characteristics of a steer-by-wire vehicle. However, they adopted linear tire-side force characteristic models. In practice, the tire-side force is nonlinear. To accurately control or predict the performance of the system, the effects of these nonlinearities should be taken into consideration. Recently, the nonlinear tire model and the stability analysis of bifurcations of a vehicle dynamic system have been proposed only in a few investigations (Catino *et al.*, 2003; Dai and Han, 2004; Ono *et al.*, 1998). However, studies of chaotic dynamics and chaotic control have not been carried out for vehicle dynamic systems. Various numerical analyses such as a bifurcation diagram, phase portraits, a Poincare map, frequency spectra and Lyapunov exponents are presented to observe periodic and chaotic motions. For a broad range of parameters, the Lyapunov exponent, which can be used to determine whether the system is in chaotic motion, offers the most powerful means of measuring the sensitivity of the dynamic system to its initial conditions. The algorithms for computing Lyapunov exponents of smooth dynamic systems are well established (Shimada and Nagashima, 1979; Wolf *et al.*, 1985; Benettin *et al.*, 1980a; Benettin *et al.*, 1980b). However, some non-smooth dynamic systems have discontinuities, such as those associated with dry friction, backlash, or impact, where this algorithm

*Corresponding author. e-mail: changsc@mail.dyu.edu.tw

cannot be directly applied. Many researchers have proposed methods for calculating the Lyapunov exponents of non-smooth dynamic systems (Muller, 1995; Hinrichs *et al.*, 1997; Stefanski, 2000). The method proposed by Stefanski (2000) for estimating the largest Lyapunov exponent for a wiper system is employed herein; the handling and the steering characteristics of a vehicle with various wheel speeds on a low-friction road are analyzed. In many engineering problems of chaos control, it is important to develop control techniques to drive a chaotic attractor to a periodic orbit. Since the pioneering work of Ott *et al.* (1990) in controlling chaos, many modified methods and other approaches have successively been proposed (Ditto *et al.*, 1990; Hunt, 1991; Lai *et al.*, 1993; Cai *et al.*, 2002a, 2002b; Fun and Tung, 1997). Dither is an external signal, so its application does not require any kind of measurement. Accordingly, the main advantage of the application of dither is its simplicity. This technique is also extensively used in several real nonlinear systems (Fun and Tung, 1997; Feeny and Moon, 2000; Liaw and Tung, 1998; Tung and Chen, 1993; Chang and Lin, 2005). Fuh and Tung (1997) used dither signals to convert a chaotic motion to a periodic orbit in circuit systems. Liaw and Tung (1998) employed the dither smoothing technique to control a noisy chaotic system. For a closed-loop DC motor system, Tung and Chen (1993) presented an approach for identifying unknown parameters and nonlinearities. The nature of a dither signal that eliminates possible limit cycles in the system was also investigated. Chang and Lin (2005) applied dither signals to suppress a chaotic electromagnetic system.

Chaotic motion must be transformed to a periodic orbit in a steady state to improve vehicle handling and steering performance. This study demonstrates that chaos can be controlled by injecting another external input, called a dither signal, into the system. The injection of dither signals to improve the performance of nonlinear elements is efficient and feasible, as verified by simulations.

2. FORMULATION OF PROBLEM

2.1. Vehicle Model

In this work, a nonlinear version of the two-degrees-of-freedom model presented in Figure 1 (Ono *et al.*, 1998) is adopted. The dynamics of lateral vehicle motion when a vehicle is running at a constant speed, v, are described. Vehicle motion in the horizontal plane is represented here using a bicycle model with states of chassis slip angle β at the center of gravity, and yaw rate γ. The lateral and yaw vehicle motion equations derived from this model with nonlinear tire-force characteristics are as follows.

Equation of lateral motion

$$mv(\dot{\beta}+\gamma) = F_f + F_r, \tag{1}$$

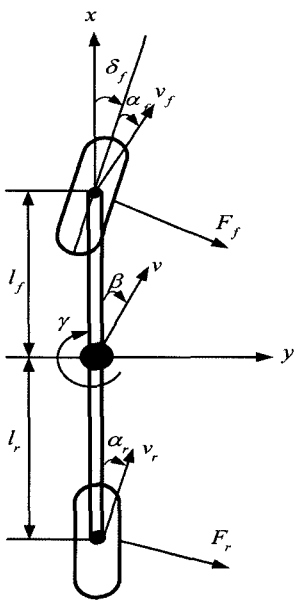

Figure 1. Model of lateral motion of vehicle.

where

β : the slip angle (rad).
γ : the yaw rate (rad/s).
F_f : the cornering force of the front two tires (N).
F_r : the cornering force of the rear two tires (N).
m : the vehicle mass (kg).
v : the vehicle velocity (m/s).

And

$$v = 2\pi RN/6000, \tag{2}$$

where

R : the radius of the wheel (cm).
N : the wheel speed (rpm).

Equation of yaw motion

$$I_z\dot{\gamma} = (l_f F_f + l_r F_r)\cos\beta, \tag{3}$$

where

l_f : the distance from the front axle to the center of gravity (m).
l_r : the distance from the rear axle to the center of gravity (m).
I_z : the yaw moment of inertia (kgm^2).

The following approximations are used for the front and rear slip angles if a slip angle β is assumed to be small.

$$\alpha_f = \beta + \tan^{-1}\left(\frac{l_f}{v}\gamma\cos\beta\right) - \delta_f$$
$$\approx \beta + \frac{l_f}{v}\gamma - \delta_f$$

$$= \beta + \frac{3000 l_f}{\pi RN}\gamma - \delta_f, \tag{4}$$

$$\alpha_r = \beta - \tan^{-1}\left(\frac{l_r}{v}\gamma\cos\beta\right)$$

$$\approx \beta - \frac{l_r}{v}\gamma$$

$$= \beta - \frac{3000 l_r}{\pi RN}\gamma, \tag{5}$$

where

α_f : the sideslip angle of the front tires (rad).
α_r : the sideslip angle of the rear tires (rad).
δ_f : the front steer angle (rad).

The correction of the dynamic behavior of the simulated vehicle depends on how accurately the tire model captures the real tire characteristics. Accordingly, researchers have developed many tire models to improve predicted tire performance. Therefore, tire forces are calculated using the well-known Magic Formula (Bakker *et al.*, 1989).

$$F_f = D_f \sin\{C_f \tan^{-1}[B_f(1-E_f)\alpha_f + E_f \tan^{-1}(B_f\alpha_f)]\}, \tag{6}$$

$$F_r = D_r \sin\{C_r \tan^{-1}[B_r(1-E_r)\alpha_r + E_r \tan^{-1}(B_r\alpha_r)]\}. \tag{7}$$

Table 1 presents the coefficients B_i, C_i, D_i and E_i, $(i = f, r)$ in the models. Front and rear cornering forces F_f and F_r are described as a nonlinear saturation function of the sideslip angles shown in Figure 2. Equations (6) and (7) are simplified to facilitate the stability analysis. Taking into account

$$\arctan z = z - \frac{z^3}{3} + \frac{z^5}{5} - \ldots,$$

$$\sin z = z - \frac{z^3}{3!} + \frac{z^5}{5!} - \ldots,$$

and neglecting high-order terms yields the simplified nonlinear tire formula,

$$F_f = k_1\alpha_f - k_2\alpha_f^3, \tag{8}$$

Table 1. Coefficients for the magic formula for a low friction road (LFR) and high friction road (HFR).

Road surface	Wheel	B_f, B_r	C_f, C_r	D_f, D_r	E_f, E_r
High friction road	Front	11.275	1.5600	2574.7	−1.9990
	Rear	18.631	1.5600	1749.7	−1.7908
Low friction road	Front	6.7651	1.3000	6436.8	−1.9990
	Rear	9.0051	1.3000	5430.0	−1.7908

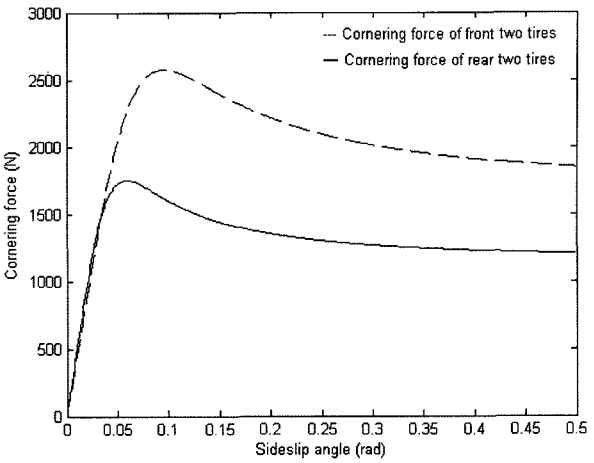

Figure 2. Cornering force characteristics.

where $k_1 = C_f B_f D_f$ and $k_2 = \frac{D_f E_f C_f B_f^3}{3} + \frac{D_f C_f B_f^3}{3} + \frac{D_f}{6}(C_f B_f)^3$,

$$F_r = k_3\alpha_r - k_4\alpha_r^3, \tag{9}$$

where $k_3 = C_r B_r D_r$ and $k_4 = \frac{D_r E_r C_r B_r^3}{3} + \frac{D_r C_r B_r^3}{3} + \frac{D_r}{6}(C_r B_r)^3$.

Equations (8) and (9) represent the cornering force used in further analysis.

2.2. Steer-by-Wire System

Because no mechanical linkage exists between the steering wheel and steering gear, the steer-by-wire system (Figure 3) has the advantage of the absence of interference between the driver's steering and the control of stability using the automatic front-wheel steering control. The steering by the driver is detected by a steering angle sensor and a torque sensor; this information is transferred to a controller, which uses this and other sensor infor-

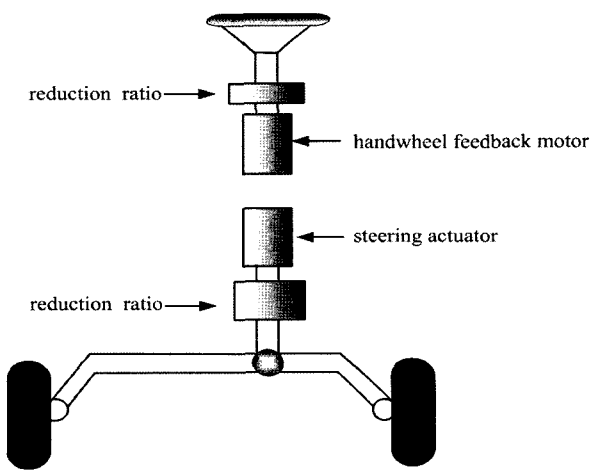

Figure 3. Steer-by-wire system.

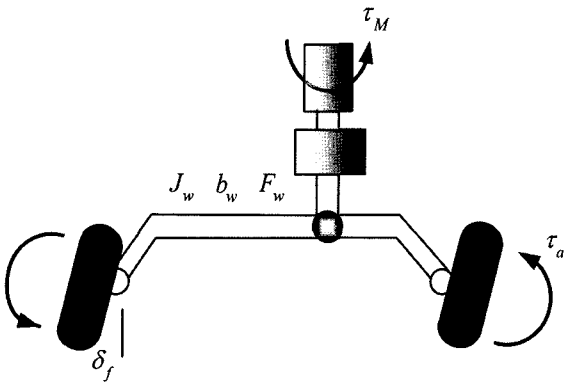

Figure 4. Steering system dynamics.

mation to control the front-wheel angle by a steering actuator. The steering actuator, which consists of a brushless DC servomotor and gear case controlled by a servo amplifier, was selected based on the maximum torque and speed required to steer the vehicle under typical driving conditions, including moderate emergency maneuvers. The steering reactive torque transmitted to the driver is controlled using a column-mounted reactive torque motor. The steer-by-wire control system, developed by Yih and Gerdes (2005), determines the current, i_M, required by the steering servomotor to follow the driver's steering commands.

The differential equation for the steering system shown in Figure 4 is as follows:

$$J_w\ddot{\delta}_f + b_w\dot{\delta}_f + \tau_f + \tau_a = r_s\tau_M, \tag{10}$$

where

δ_f : the front steering angle (rad).
J_w : the total moment of inertia of the system (Nms^2/rad).
b_w : viscous damping (Nms/rad).
τ_f : coulomb friction (Nm).
τ_a : the self-aligning moment of the tire (Nm).
r_s : the steering ratio.

τ_M is the motor torque, which can be expressed in terms of the motor constant, k_M, the motor current, i_M, and the motor efficiency, η:

$$\tau_M = k_M i_M \eta. \tag{11}$$

The tire self-aligning moment, τ_a, is a function of the steering geometry, in particular the caster angle, and the manner in which the tire deforms to generate lateral forces. In Figure 5, F_f is the cornering force of the front two tires; α_f is the tire sideslip angle; t_p (m) is the pneumatic trail, which is the distance between the resultant point of application of the lateral force and the center of the tire; t_m (m) is the mechanical trail, which is the distance between the center of the tire and the steering axis, and v is the velocity of the center of the tire. The

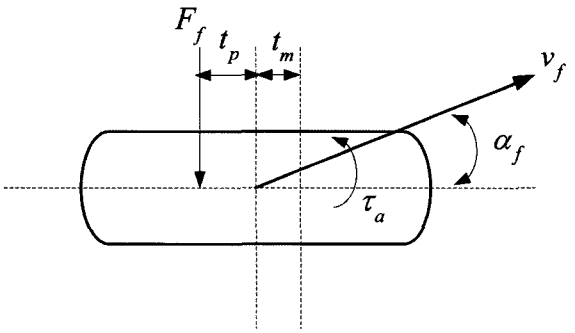

Figure 5. Tire self-aligning torque at a sideslip angle.

total aligning moment is given by,

$$\tau_a = (t_p + t_m)F_f. \tag{12}$$

The resisting torque, τ_f, is treated as

$$\tau_f = 9.8 t_p \mu F_w \operatorname{sgn}(\dot{\delta}_f), \tag{13}$$

where μ is the coefficient of friction and F_w (kg) is the weight on the front wheel.

Taking into account the above considerations and setting $x_1=\beta$, $x_2=\gamma$, $x_3=\delta_f$, and $x_4=\dot{\delta}_f$ yields the following state-space models with combined dynamics of the vehicle chassis and the steering system:

$$\dot{x}_1 = \frac{3000(F_f + F_r)}{\pi m R N} - x_2,$$

$$\dot{x}_2 = \frac{l_f F_f - l_r F_r}{I_z},$$

$$\dot{x}_3 = x_4,$$

Table 2. Parameter values of the vehicle and steering system model.

System parameter	Value	Unit
m	1500	kg
R	30	cm
I_Z	2000	kgm^2
l_f	1.2	m
l_r	1.3	m
J_w	10	Nms^2/rad
b_w	200	Nms/rad
r_s	30	
k_M	0.078	Nm/A
i_M	10	A
η	0.7	
t_p	0.012	m
t_m	0.010	m
F_w	200	kg

$$\dot{x}_4=\frac{-b_w x_4}{J_w}+\frac{r_s \tau_M}{J_w}-\frac{\tau_f}{J_w}-\frac{\tau_a}{J_w}. \quad (14)$$

Table 2 presents the values of the parameters in the above equations.

3. ESTIMATION OF THE LARGEST LYAPUNOV EXPONENT AND NUMERICAL SIMULATION RESULTS

The largest Lyapunov exponent is one of the most useful diagnostic indicators of a chaotic system. Every dynamic system has a spectrum of Lyapunov exponents (λ) that determines how the lengths, areas and volumes change in phase space. In other words, Lyapunov exponents measure the rate of divergence (or convergence) of two initial nearby orbits. Chaos can be identified by simply calculating the largest Lyapunov exponent, thus determining whether nearby trajectories diverge ($\lambda > 0$) or converge ($\lambda < 0$) on average. Any bounded motion in a system that contains at least one positive Lyapunov exponent is defined as chaotic, while non-positive Lyapunov exponents indicate periodic motion.

Algorithms for computing the Lyapunov spectrum of "smooth" dynamic systems are well established (Wolf *et al.*, 1985; Benettin *et al.*, 1980a, 1980b). However, "non-smooth" dynamic systems with discontinuities such as dry friction, backlash or stick-slip prevent this algorithm from being applied directly. Stefanski (2000) recently recommended a simple method for estimating the largest Lyapunov exponent based on the synchronization characteristics. The synchronization of two distinct systems that may have identical structures or be completely different has recently attracted particular interest. Synchronization controls the response system using the output of the drive system, so the output of the response system asymptotically follows the output of the drive system.

Stefanski's method for estimating the largest Lyapunov exponent is briefly described herein, and the calculations are described in detail (Stefanski, 2000). The basic procedures of this technique follow.

The dynamic system is decomposed into the following two subsystems:

drive system

$$\dot{x}=f(x), \quad (15)$$

and response system

$$\dot{y}=f(y). \quad (16)$$

Consider a dynamic system that is composed of two identical n-dimensional subsystems; a coupling coefficient, d, is applied only to the response system (16), while the drive equation remains unchanged. The first-order differential equations for such a system can be expressed as

$$\dot{x}=f(x),$$
$$\dot{y}=f(y)+d(x-y). \quad (17)$$

The condition of synchronization (Equation (17)) is given by the inequality,

$$d > \lambda_{\max}. \quad (18)$$

The smallest value of the coupling coefficient d in the synchronization, d_s, is assumed to equal the maximum Lyapunov exponent

$$d_s=\lambda_{\max}. \quad (19)$$

Equation (17) yields the augmented system, based on Equation (14), as follows.

$$\dot{x}_1=\frac{3000(F_f+F_r)}{\pi mRN}-x_2,$$

$$\dot{x}_2=\frac{l_f F_f-l_r F_r}{I_z},$$

$$\dot{x}_3=x_4,$$

$$\dot{x}_4=\frac{-b_w x_4}{J_w}+\frac{r_s \tau_M}{J_w}-\frac{\tau_f}{J_w}-\frac{\tau_a}{J_w}.$$

$$\dot{y}_1=\frac{3000(\tilde{F}_f+\tilde{F}_r)}{\pi mRN}-y_2+d(x_1-y_1),$$

$$\dot{y}_2=\frac{l_f \tilde{F}_f-l_r \tilde{F}_r}{I_z}+d(x_2-y_2),$$

$$\dot{y}_3=x_4+d(x_3-y_3),$$

$$\dot{y}_4=\frac{-b_w y_4}{J_w}+\frac{r_s \tau_M}{J_w}-\frac{\tau_f}{J_w}-\frac{\tau_a}{J_w}+d(x_4-y_4), \quad (20)$$

where $\tilde{\alpha}_f=y_1+\frac{3000 l_f}{\pi RN}y_2-y_3$, $\tilde{\alpha}_r=y_1-\frac{3000 l_r}{\pi RN}y_2$, $\tilde{F}_f=k_1\tilde{\alpha}_f-k_2\tilde{\alpha}_r^3$, and $\tilde{F}_r=k_3\tilde{\alpha}_r-k_4\tilde{\alpha}_r^3$.

In the next step, following the method described above, the largest value of the Lyapunov exponent of the system under consideration is determined for the chosen parametric values. Figure 6 presents the results of the numerical calculations, which reveal the largest Lyapunov exponents that have been obtained using the described synchronization method. The system exhibits chaotic motion because all of the largest Lyapunov exponents are positive for 1645 rpm $< N <$ 1825 rpm and $N >$ 1855 rpm.

A series of numerical simulations from Equation (14) were performed to understand clearly the characteristics of this system. The purpose of the numerical study is to find some sets of parameters that lead to chaotic motion. A widely employed technique for determining the responses in a dynamic system under parametric variations is the bifurcation diagram. The dynamic behaviors may be observed more completely over a range of parameter values using the bifurcation diagram, as shown in Figure

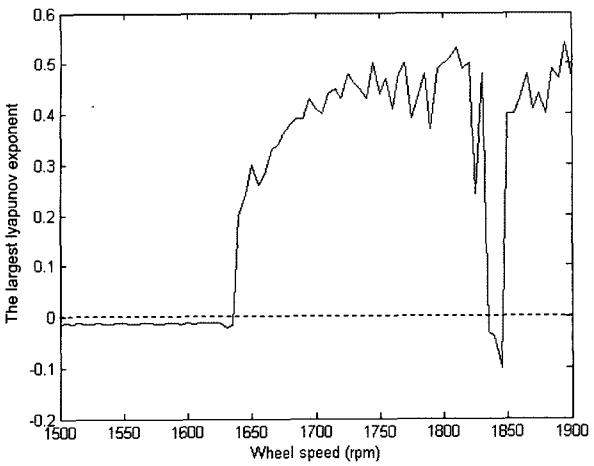

Figure 6. Evolutions of the largest Lyapunov exponent.

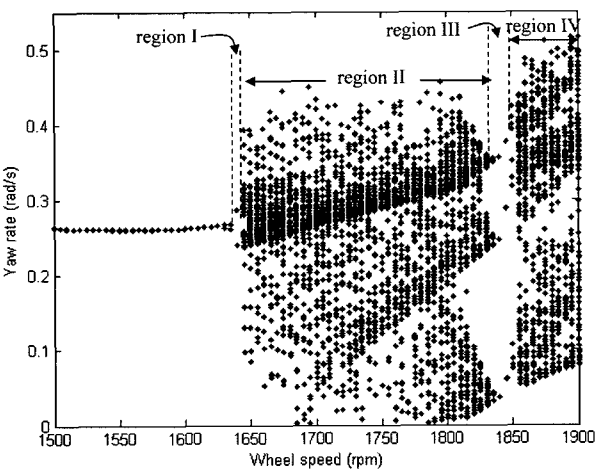

Figure 7. Bifurcation diagram of wheel speed N versus yaw rate γ.

7. The figure clearly shows that the motion is chaotic approximately in regions II and IV because all of the largest Lyapunov exponents are positive for the two regions. Period-2 motion appears in region I and Period-3 motion exists in region III. These behaviors are described in detail in the phase portrait, Poincare map and frequency spectrum, which are presented in this author's previous work (Chang, 2007).

4. CONTROLLING CHAOS BY INJECTING DITHER SIGNALS

Although nonlinear behavior in a control system may be acceptable, it is undesirable since it can cause performance deprivation and even instability. In order to relieve these problems, it is sometimes practicable to make the nonlinear elements more approximately linear in effect, by causing the operating point to sweep repeatedly over a certain range around its nominal position. This is done by adding another external input, called a dither signal, into the system just ahead of the nonlinearity (Cook, 1986). This section will demonstrate that the injection into this chaotic system of a dither signal, an external input which only affects the nonlinear terms, can control the chaotic motion. Using the dither signal method, a chaotic motion can be converted to a periodic orbit or a steady state, depending on the system input. Dither is a high-frequency signal applied to modify the behaviors of any system with friction. The main use of dither in a system is to modify nonlinearity. Recently, dither-smoothing techniques have been developed (Fun and Tung, 1997; Liaw and Tung, 1998; Chang and Lin, 2005) to stabilize the chaotic systems. Some popular dither signals follow (Cook, 1986).

(i) Square-wave dither: The simplest dither signal is a square-wave dither, whose frequency and amplitude are 2000 rad/s and W, respectively. Thus, the non-linearity $f(.)$ has the effective value output

$$n=\frac{1}{2}[f(y+W)+f(y-W)]. \tag{21}$$

Accordingly, the system equations can be written as

$$\dot{y}=n. \tag{22}$$

Consider the effect of the addition of square-wave dither control to the system equation, Equation (14) for N = 1750 rpm. Increasing the amplitude of the square-wave dither signal from $W = 0$ to 0.14 V changes the dynamics from chaotic behavior to periodic. The bifurcation diagram is shown in Figure 8. Consider the nonlinear lateral force of the front wheels, F_f, the nonlinear lateral force of the rear wheels, F_r, and the resisting torque, τ_f, which are all originally associated with nonlinearity f as described in Equations (8), (9), and (13), respectively.

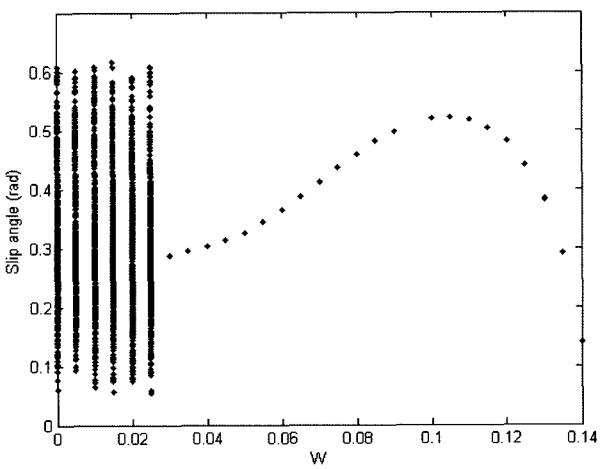

Figure 8. Bifurcation diagram of system with square-wave dither, where W denotes the amplitude of the dither.

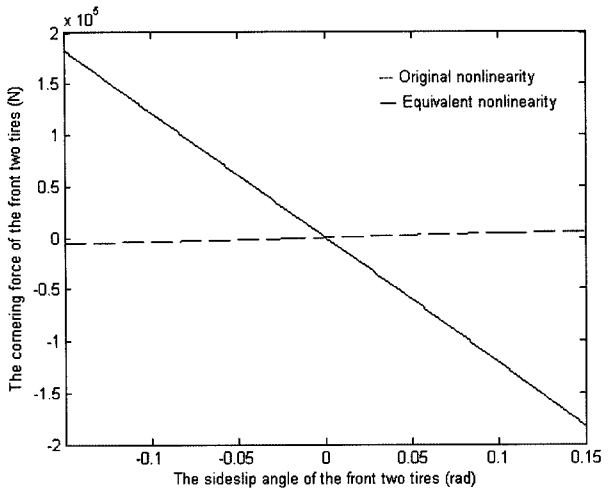

Figure 9. Equivalent nonlinearity n (solid line) described by Equation (21). The original nonlinearity f (dashed line) is given by Equation (8).

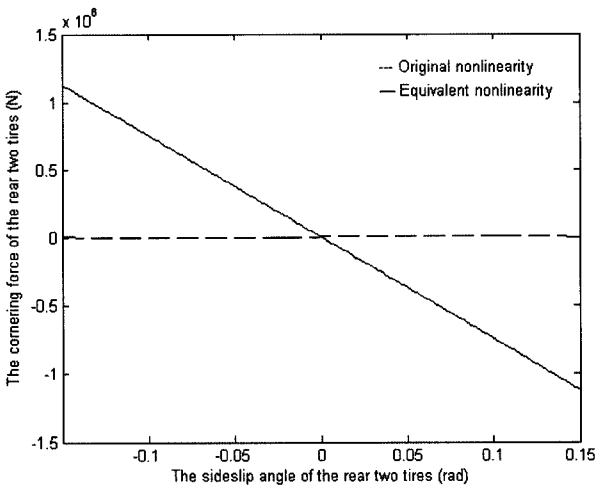

Figure 10.Equivalent nonlinearity n (solid line) described by Equation (21). The original nonlinearity f (dashed line) is given by Equation (9).

Now, $W = 0.1$ V is chosen and the effective nonlinearity and original nonlinearity plotted in Figures 9, 10, and 11. Figure 12(a) shows the phase portrait of the controlled system. Figure 12(b) plots the time response of the slip angle, where the square-wave dither signal is injected after 3 s. The chaotic behavior is converted into a period-one motion.

(ii) Sinusoidal dither: Another simple dither signal is a high-frequency sinusoid. In this case, the effective value of n is its average over a complete period of oscillation of the sinusoidal dither signal, namely

$$n=\frac{1}{2\pi}\int_0^{2\pi} f(x + W\sin\theta)d\theta. \tag{23}$$

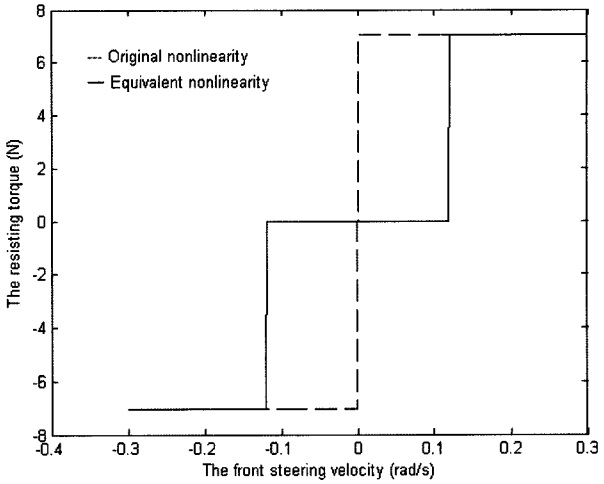

Figure 11. Equivalent nonlinearity n (solid line) described by Equation (21). The original nonlinearity f (dashed line) is given by Equation (13).

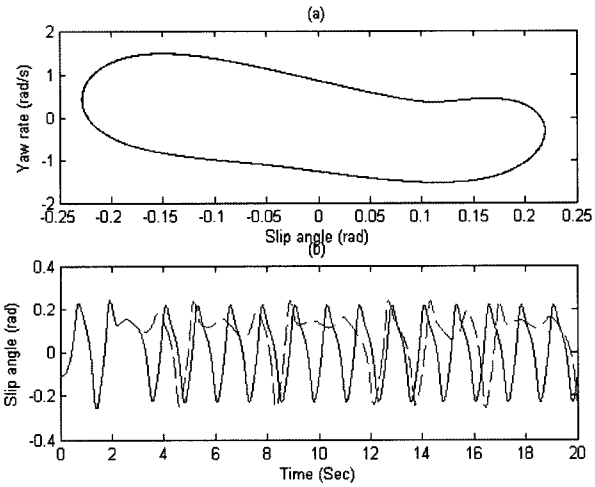

Figure 12. A square-wave dither signal is injected to control the chaotic motion of the system at N = 1750 (rpm). A dither signal ($W = 0.1$ V) is added after 3 s. (a) Phase portrait of desired period-one orbit; (b) time response of the slip angle. The solid line represents the corresponding period-one of the controlled system (22); the dotted line represents the chaotic trajectory of the uncontrolled system (14).

Now, a sinusoidal dither is added in front of the nonlinearity. The equivalent equations for the control system are shown below.

Adding the sinusoidal dither signal to Equation (14) yields a coupled system:

$$\dot{x}_1=\frac{3000(n_1 + n_2)}{\pi mRN}-x_2,$$

$$\dot{x}_2=\frac{l_f n_1 - l_r n_2}{I_z},$$

$$\dot{x}_3=x_4,$$

$$\dot{x}_4=\frac{-b_w x_4}{J_w}+\frac{r_s \tau_M}{J_w}-\frac{n_3}{J_w}-\frac{\tau_a}{J_w}, \tag{24}$$

Where

$$n_1=\frac{1}{2\pi}\int_0^{2\pi} F_f(\alpha_f + W\sin\theta)d\theta \tag{25}$$
$$=\frac{1}{2\pi}\int_0^{2\pi}[k_1(\alpha_f + W\sin\theta)-k_2(\alpha_f + W\sin\theta)^3]d\theta,$$

$$n_2=\frac{1}{2\pi}\int_0^{2\pi} F_r(\alpha_r + W\sin\theta)d\theta \tag{26}$$
$$=\frac{1}{2\pi}\int_0^{2\pi}[k_3(\alpha_r + W\sin\theta)-k_4(\alpha_r + W\sin\theta)^3]d\theta,$$

$$n_3=\frac{1}{2\pi}\int_0^{2\pi} \tau_f(\delta_f + W\sin\theta)d\theta \tag{27}$$
$$=\frac{1}{2\pi}\int_0^{2\pi}[9.8 t_p \mu F_w \mathrm{sgn}(\dot{\delta}_f + W\sin\theta)]d\theta,$$

The dither frequency must be much greater than any other involved in the operation of the system. Otherwise, the dither signal may introduce another undesirable oscillation with the same frequency as the dither signal. Now, set the system parameter N to 1750 rpm and the frequency of the sinusoidal dither to 4000 rad/s. The resulting bifurcation diagram, shown in Figure 13, reveals that a sinusoidal dither with amplitude from 0.8 to 1.2 V can convert the chaotic motion of the automotive wiper system to period-one motion. Now, set the sinusoidal dither amplitude W to 1.0 V and frequency to 4000 rad/s, and add this signal in front of the nonlinearity, Equations (8), (9), and (13). The results of the equivalent nonlinearity are shown in Figures 14, 15, and 16 (the effective nonlinearity versus the original nonlinearity). In the simulations, W = 1.0 V is set and the dither signal applied after 3 s. Figure 17 plots the results. As can be seen, the system exhibits a chaotic behavior before the dither is applied, whereas it exhibits a periodic motion thereafter. A sinusoidal dither with amplitude W = 1.0 V, frequency = 4000 rad/s is injected after 3 s to convert the dynamics of system, Equation (14), from chaotic motion to periodic motion. Figure 17(a) shows the phase portrait of the system after control. Figure 17(b) plots the time response of slip angle, with the dither control added after 3 s. Before the dither is applied, the system exhibits a chaotic

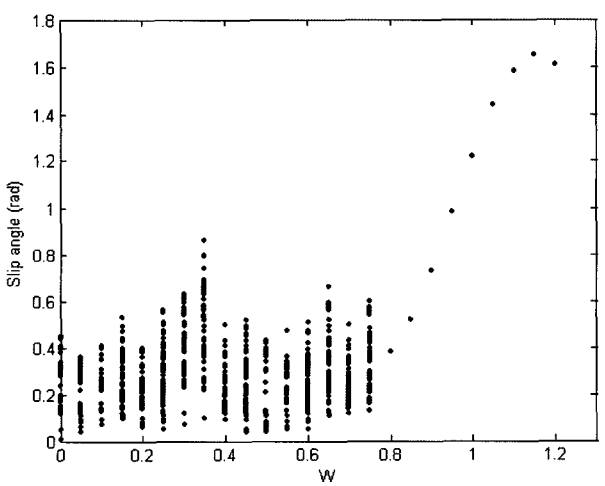

Figure 13. Bifurcation diagram of system with sinusoidal dither, where W denotes the amplitude of the dither.

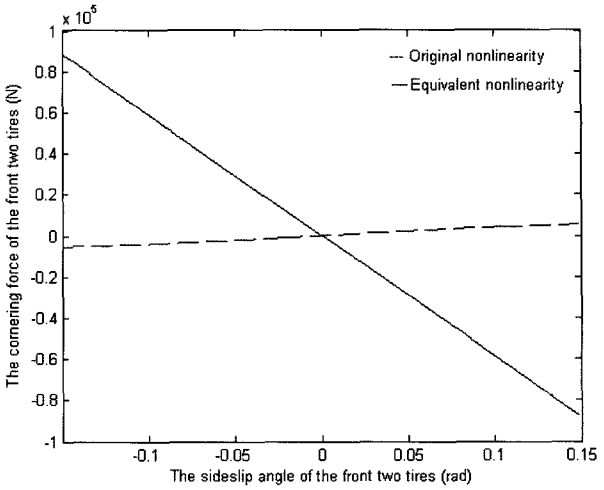

Figure 14. Equivalent nonlinearity n_1 (solid line) described by Equation (25). The original nonlinearity f (dashed line) is given by Equation (8).

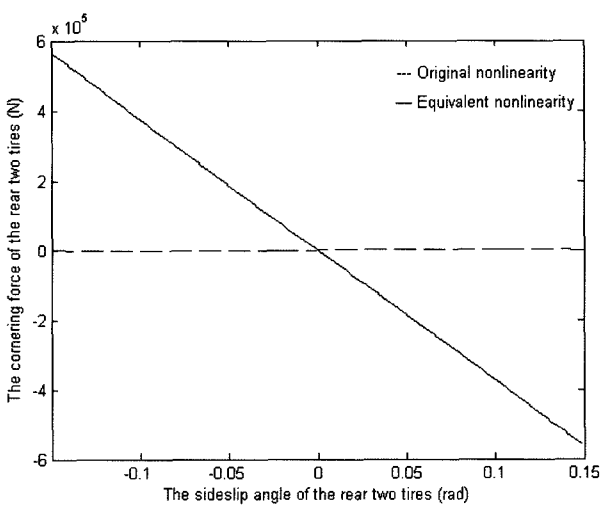

Figure 15. Equivalent nonlinearity n_2 (solid line) described by Equation (26). The original nonlinearity f (dashed line) is given by Equation (9).

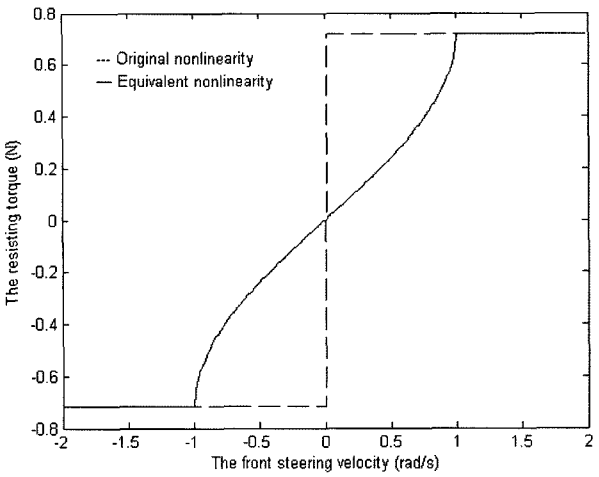

Figure 16. Equivalent nonlinearity n_3 (solid line) described by Equation (27). The original nonlinearity f (dashed line) is given by Equation (13).

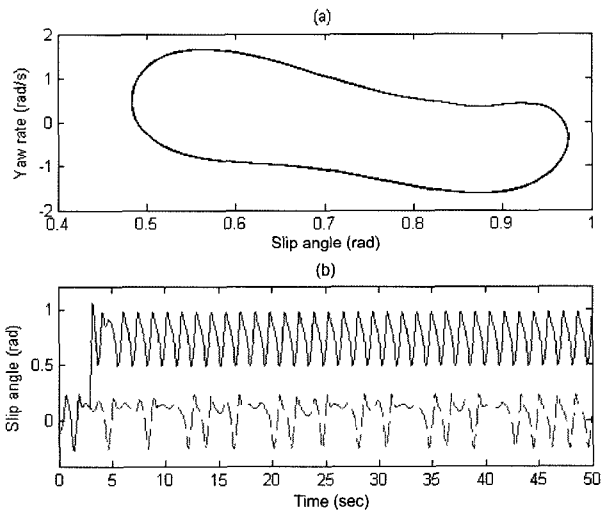

Figure 17. Controlling chaotic motion and converting it to a desired period-one orbit for $W = 1.0$ V and $N = 1750$ (rpm). The sinusoidal dither signal is injected after 3 s. (a) Phase portrait of desired period-one orbit; (b) time response of the slip angle. The solid line represents the corresponding period-one of the controlled system (24); the dotted line represents the chaotic trajectory of the uncontrolled system (14).

behavior; afterward, it exhibits periodic behavior.

5. CONCLUSIONS

This study addresses complex nonlinear behaviors and control of chaotic dynamics of vehicles with a steer-by-wire system. The dynamic behaviors can be observed over a range of parameter values using the bifurcation diagram. This diagram reveals that the vehicle's dynamic system is chaotic at a high wheel speed on a low-friction road. The Lyapunov exponent is a very powerful tool for determining whether a system exhibits chaotic motion. The largest Lyapunov exponent of the vehicle handling and steer-by-wire system was estimated from its synchronization properties. Finally, square-wave and sinusoidal dither signals can, when injected in front of the nonlinearity of a chaotic system, efficiently convert the chaotic system into a periodic orbit and improve the performance of the vehicle handling and the steering system.

ACKNOWLEDGMENTS–The author would like to thank the National Science Council of the Republic of China, Taiwan, for financially supporting this research under Contract No. NSC 94-2218-E-212-006.

REFERENCES

Ackermann, J. and Sienel, W. (1993). Robust yaw damping of cars with front and rear wheel steering. *IEEE Trans. Control Systems Technology,* **1**, 15–20.

Bakker, E., Pacejka, H. B. and Lidner, L. (1989). A new tire model with an application in vehicle dynamics studies. *Proc. Int. Congress and Exposition, SAE Paper No.* 890087.

Benettin, G., Galgani, L., Giorgilli, A. and Strelcyn, J. M. (1980a). Lyapunov exponents for smooth dynamical systems and hamiltonian systems; a method for computing all of them. *Part I: Theory, Meccanica,* **15**, 9–20.

Benettin, G., Galgani, L., Giorgilli, A. and Strelcyn, J. M. (1980b). Lyapunov exponents for smooth dynamical systems and hamiltonian systems; A method for computing all of them. *Part II: Numerical Application, Meccanica,* **15**, 21–30.

Catino, B., Santini, S. and Bernardo, M. D. (2003). MCS adaptive control of vehicle dynamics: an application of bifurcation techniques to control system design. *IEEE 42nd Conf. Decision Contr.*, 2252–2256.

Cai, C., Xu, Z., Xu, W. and Feng, B. (2002a). Notch filter feedback control in a class of chaotic systems. *Automatica,* **38**, 695–701.

Cai, C., Xu, Z. and Xu, W. (2002b). Converting chaos into periodic motion by feedback control. *Automatica,* **38**, 1927–1933.

Chang, S. C. and Lin, H. P. (2005). Nonlinear dynamics and chaos control for an electromagnetic system. *J. Sound and Vibration,* **279**, 327–344.

Chang, S. C. (2007) Adoption of state feedback to control dynamics of vehicle with steer-by-wire system. *Proc. Institution of Mechanical Engineers, Part D: J. Automobile Engineering,* **221**, 1–12.

Cook, P. A. (1986). *Nonlinear Dynamical Systems.* Pren-

tice-Hall. Englewood Cliffs.

Dai, L. and Han, Q. (2004). Stability and hopf bifurcation of a nonlinear model for a four-wheel-steering vehicle system. *Communications in Nonlinear Science and Numerical Simulation,* **9**, 331–341.

Ditto, W. L., Rauseo, S. N. and Spano, M. L. (1990). Experimental control of chaos. *Physical Review Letters,* **65**, 3211–3214.

Feeny, B. F. and Moon, F. C. (2000). Quenching stick-slip chaos with dither. *J. Sound and Vibration,* **273**, 173–180.

Fun, C. C. and Tung, P. C. (1997). Experimental and analytical study of dither signals in a class of chaotic system. *Physics Letters, A* **229**, 228–234.

Harada, M. and Harada, H. (1999). Analysis of lateral stability with integrated control of suspension and steering systems. *JSAE Review,* **20**, 465–470.

Hayama, R. and Nishizaki, K. (2000). The vehicle stability control responsibility improvement using steer-by-wire. *Proc. IEEE Intelligent Vehicles Symp.*, 596–601.

Hinrichs, N., Oestreich, M. and Popp, K. (1997). Dynamics of oscillators with impact and friction. *Chaos, Solitons & Fractals,* **8**, 535–558.

Hosaka, M. and Murakami, T. (2004). Yaw rate control of electric vehicle using steer-by-wire system. *IEEE 8th Int. Workshop, Advance Motion Control,* 31–34.

Hunt, E. R. (1991). Stabilizing high-period orbits in a chaotic system: The diode resonator. *Physical Review Letters,* **67**, 1953–1955.

Lai, Y. C., Ding, M. and Grebogi, C. (1993). Controlling hamiltonian chaos. *Physical Review,* E **67**, 86–92.

Liaw, Y. M. and Tung, P. C. (1998). Application of the differential geometric method to control a noisy chaotic system via dither smoothing. *Physics Letters,* A **239**, 51–58.

Muller, P. (1995). Calculation of Lyapunov exponents for dynamical systems with discontinuities. *Chaos, Solitons & Fractals,* **5**, 1671–1681.

Ono, E., Hosoe, S., Tuan, H. D. and Doi, S. (1998). Bifurcation in vehicle dynamics and robust front wheel steering control. *IEEE Trans. Control Systems Technology,* **6**, 412–420.

Ott, E., Grebogi, C. and Yorke, J. A. (1990). Controlling chaos. *Physical Letters,* **64**, 1196–1199.

Sano, S., Furukawa, Y. and Siraishi, S. (1986). Four wheel steering system with rear wheel steer angle controlled as function of steering wheel angle. *Proc. Int. Cong. and Exposition, SAE Paper No.* 860625.

Segawa, M., Nakano, S., Nishihara, O. and Kumamoto, H. (2001). Vehicle stability control strategy for steer by wire system. *JSAE Review,* **22**, 383–388.

Setlur, P., Dawson, D., Wagner, J. and Fang, Y. (2002). Nonlinear tracking controller design for steer-by-wire automotive systems. *Proc. American Control Conf. Anchorage*, 280–285.

Shibahata, Y., Irie, N., Itoh, H. and Nakamura, K. (1986). The development of an experimental four-wheel-steering vehicle. *Proc. Int. Congress and Exposition, SAE Paper No.* 860623.

Shimada, I. and Nagashima, T. (1979). A numerical approach to ergodic problems of dissipative dynamical systems. *Progress of Theoretical Physics,* **61**, 1605–1616.

Stefanski, A. (2000). Estimation of the largest Lyapunov exponent in systems with impact. *Chaos, Solitons & Fractals,* **11**, 2443–2451.

Takiguchi, T., Yasuda, N., Furutani, S., Kanazawa, H. and Inoue, H. (1986). Improvement of vehicle dynamics by vehicle-speed-sensing four-wheel steering system. *Proc. Int. Congress and Exposition, SAE Paper No.* 860624.

Tung, P. C. and Chen, S. C. (1993). Experimental and analytical studies of the sinusoidal dither signal in a dc motor system. *Dynamics and Control,* **3**, 53–69.

Wolf, A., Swift, J. B., Swinney, H. L. and Vastano, J. A. (1985). Determining Lyapunov exponents from a time series. *Physica,* D **16**, 285–317.

Yih, P. and Gerdes, J. C. (2005). Modification of vehicle handling characteristics via steer-by-wire. *IEEE Trans. Control Systems Technology,* **13**, 965–976.

You, S. S. and Jeong, S. K. (2002). Controller design and analysis for automatic steering of passenger cars. *Mechatronics,* **12**, 427–446.